frontiers | Frontiers in Marine Science

TYPE Original Research
PUBLISHED 17 October 2023
DOI 10.3389/fmars.2023.1196938

OPEN ACCESS

EDITED BY
Jose Martin Hernandez-Ayon,
Autonomous University of Baja California, Mexico

REVIEWED BY
Zvi Steiner,
Helmholtz Association of German Research Centres (HZ), Germany
Galdies Galdies,
University of Malta, Malta
Eva Krasakopoulou,
University of the Aegean, Greece

*CORRESPONDENCE
I. Emma Huertas
emma.huertas@csic.es

RECEIVED 30 March 2023
ACCEPTED 12 September 2023
PUBLISHED 17 October 2023

CITATION
Amaya-Vías S, Flecha S, Pérez FF, Navarro G, García-Lafuente J, Makaoui A and Huertas IE (2023) The time series at the Strait of Gibraltar as a baseline for long-term assessment of vulnerability of calcifiers to ocean acidification. *Front. Mar. Sci.* 10:1196938. doi: 10.3389/fmars.2023.1196938

The time series at the Strait of Gibraltar as a baseline for long-term assessment of vulnerability of calcifiers to ocean acidification

Silvia Amaya-Vías[1], Susana Flecha[2], Fiz F. Pérez[3], Gabriel Navarro[1], Jesús García-Lafuente[4], Ahmed Makaoui[5] and I. Emma Huertas[1]*

[1]Instituto de Ciencias Marinas de Andalucía, Consejo Superior de Investigaciones Cientificas (CSIC), Cádiz, Spain, [2]Instituto Mediterráneo de Estudios Avanzados (IMEDEA), Esporles, Mallorca, Spain, [3]Instituto de Investigaciones Marinas, Consejo Superior de Investigaciones Cientificas (CSIC), Vigo, Spain, [4]Grupo de Oceanografía Física, Instituto de Biotecnología y Desarrollo Azul (IBYDA), Universidad de Málaga, Málaga, Spain, [5]Institut National de Recherche Halieutique (INRH), Casablanca, Morocco

The assessment of the saturation state (Ω) for calcium carbonate minerals (aragonite and calcite) in the ocean is important to determine if calcifying organisms have favourable or unfavourable conditions to synthesize their carbonated structures. This parameter is largely affected by ocean acidification, as the decline in seawater pH causes a decrease in carbonate ion concentration, which in turn, lowers Ω. This work examines temporal trends of seawater pH, $\Omega_{Aragonite}$ and $\Omega_{Calcite}$ in major Atlantic and Mediterranean water masses that exchange in the Strait of Gibraltar: North Atlantic Central Water (NACW), Levantine Intermediate Water (LIW) and Western Mediterranean Deep Water (WMDW) using accurate measurements of carbonate system parameters collected in the area from 2005-2021. Our analysis evidences a gradual reduction in pH in the three water mases during the monitoring period, which is accompanied by a decline in Ω for both minerals. The highest and lowest decreasing trends were found in the NACW and LIW, respectively. Projected long-term changes of Ω for future increases in atmospheric CO_2 under the IPCC AR6 Shared Socio-economic Pathway "fossil-fuel-rich development" (SSP5-8.5) indicate that critical conditions for calcifiers with respect to aragonite availability will be reached in the entire water column of the region before the end of the current century, with a corrosive environment (undersaturation of carbonate) expected after 2100.

KEYWORDS

aragonite, calcite, ocean acidification, saturation state, Strait of Gibraltar

1 Introduction

The ocean plays a significant role as a sink for anthropogenic carbon dioxide (CO_2) (Sarmiento and Gruber, 2002; Le Quéré et al., 2015), absorbing approximately a quarter of the CO_2 emitted by humans to the atmosphere (Friedlingstein et al., 2022; Gruber et al., 2023). This marine contribution to CO_2 withdrawal mitigates climate change, albeit at a cost to the ecosystem, causing significant alterations in seawater chemistry (Orr et al., 2005; Doney et al., 2009; Gledhill et al., 2015).

When the CO_2 molecule enters the ocean, it hydrates and forms carbonic acid, which is a weak acid that tends to dissociate water producing hydrogen ions. As a result, the concentration of hydrogen ions ($[H^+]$) in the seawater increases steadily and slowly, leading to ocean acidification (OA) over a long period of time, i.e. a decline in the pH (Raven et al., 2005; Impacts, 2014; Williamson and Widdicombe, 2017; Doney et al., 2020). In addition, part of these $[H^+]$ bind to the carbonate ions (CO_3^{2-}) to generate bicarbonate (HCO_3^-), causing a decrease in the concentration of CO_3^{2-} and, consequently, their availability in the medium. Carbonate ions are essential for marine calcifying organisms to form their skeletons and shells, and their decline severely affects the biogenic calcification process (Riebesell et al., 2000; Orr et al., 2005; Feely et al., 2012; Kroeker et al., 2013; Pörtner et al., 2014; Mostofa et al., 2016; Doney et al., 2020), as marine organisms must combine Ca^{2+} and CO_3^{2-} to precipitate $CaCO_3$ for calcareous shells formation (Silverstein, 2022) (Equation 1):

$$Ca^{2+}(aq) + CO_3^{2-}(aq) \rightleftharpoons CaCO_3(s) \quad (1)$$

Calcification ability can be assessed through the estimation of the saturation state (Ω) of calcium carbonate minerals, which is defined as shown in Equation 2:

$$\Omega = \frac{[Ca^{2+}] \cdot [CO_3^{2-}]}{K'_{sp}} \quad (2)$$

where $[Ca^{2+}]$ and $[CO_3^{2-}]$ are the concentrations of calcium and carbonate ions, respectively, and K'_{sp} is the apparent solubility product for aragonite or calcite, the polymorphic mineral forms of $CaCO_3$ in the ocean. This dimensionless parameter largely depends on temperature (T), salinity (S), and pressure (P) in the medium. Values of Ω for calcite ($\Omega_{Calcite}$) and aragonite ($\Omega_{Aragonite}$) higher than 1 indicate supersaturation, i.e. favourable conditions for calcification to proceed whereas, values of Ω lower than 1 denote undersaturation and thus, corrosive conditions for calcifiers (Doney et al., 2009).

Nevertheless, biogenic calcification is also affected by other factors, such as the ability of certain organisms to regulate their internal chemistry or the presence of protective organic covers (Miller et al., 2009; Pan et al., 2015; Melzner et al., 2020). Several studies have reported reductions in calcification rates of certain organisms even when Ω exceeds 1; for instance, in some corals when Ω is comprised within the range 2-3.5 (Guinotte et al., 2003; Yamamoto et al., 2012; Eyre et al., 2018). In fact, a value equal to 1.5 for Ω in both minerals, has been considered to define negative consequences for marine ecosystems even at planetary scale (Gruber et al., 2012; Broadgate et al., 2013; Ekstrom et al., 2015; Zhai, 2018) and it has been adopted as a critical threshold for calcification to occur properly.

As OA is strengthening and it will keep increasing over the 21st century at rates dependent on future CO_2 emissions, biogenic calcification will continue being at risk. However, the magnitude of OA is not homogeneous worldwide and certain areas are more affected than others (Gattuso et al., 2015). In particular, some regions in the North Atlantic and the Mediterranean Sea (MedSea) have been found to be highly sensitive to OA (Fontela et al., 2020) and noticeable gradual decreases in seawater pH have been measured over time in Atlantic and Mediterranean water masses surrounding the southern Iberian Peninsula (Flecha et al., 2015; Flecha et al., 2019). Therefore, it can be anticipated that the saturation state of calcium carbonate minerals in this area is being affected by the progressive OA process already documented. This assumption can be tested by assessing the temporal trend of Ω in waters of the Strait of Gibraltar (SoG), the only connection between the Atlantic Ocean and the MedSea. The SoG holds a two-way exchange, with a surface inflow of Atlantic water (AI) that moves eastwards, and a compensating westward deep outflow of Mediterranean water (MOW) underneath. The AI is primarily formed by the North Atlantic Central Water (NACW) whereas the colder and saltier MOW consists of, mainly, two water masses, the Levantine Intermediate Water (LIW) and the Western Mediterranean Deep Water (WMDW). The former is the result of the transformation process undertaken by the Atlantic surface water as it moves eastward, which makes it saltier, until it sinks to intermediate depths in the Levantine basin, the easternmost basin of the MedSea (Lascaratos, 1993). In contrast, the WMDW is formed in the western Mediterranean basin, as a result of the winter cooling of highly modified surface waters in the Gulf of Lions (MEDOC Group, 1970; Fourrier et al., 2022). Both water masses flow at depth towards the SoG and leave the MedSea, merging in the MOW in the Gulf of Cádiz. Recent estimates indicate that the median transit time of the WMDW from the Gulf of Lions to the SoG is 5 years whereas the LIW takes roughly 8 years from the Strait of Sicily to the SoG (Vecchioni et al., 2023). Furthermore, the transit time of the LIW from its formation basin to the Sicily channel ranges between 8 and 13 years, depending on the approach (Roether et al., 1998; Gačić et al., 2013). Similarly, Gačić et al. (2013) based on salinity anomalies estimated that the total time interval needed for the signal propagating from the Levantine basin to reach the deep mixed layers of the Algero-Provençal sub-basin is about 25 years. Thus, the LIW identified in the SoG has crossed a larger distance and, consequently, is older and biogeochemically more stable than the WMDW also present in the area (Flecha et al., 2019 and referenes therein). Therefore, the three water masses (NACW, LIW and WMDW) found in the SoG are characterized by well-differentiated thermohaline and biogeochemical properties and history, making the channel a very suitable spot for the assessment of Ω in them.

In this study, we used periodic high-quality measurements of the carbonate system parameters collected in the SoG during 17 years of measurements (2005-2021) to accurately determine the temporal evolution of Ω in Atlantic and Mediterranean water

masses. Furthermore, as the projected changes in availability of CO_3^{2-} in the ocean due to OA would be essentially irreversible on centennial time scales (Mathesius et al., 2015; Heinze et al., 2021), long-term trends of Ω were also assessed under the IPCC AR6 scenario of fossil-fuel-rich development (SSP5-8.5) (IPCC et al., 2021). The calculated projections are finally used to infer approximately when communities of calcifying organisms would be exposed to waters undersaturated for calcium carbonate minerals in this key oceanographic region.

2 Materials and methods

2.1 Study area and sampling procedure

Data used in this study were collected during 34 oceanographic campaigns (Table 1S) conducted between 2005 and 2021 in the SoG (Figure 1), the relatively shallow (mean depth of ~600 m, with a minimum depth of 300 m in Camarinal sill or G2 in Figure 1) and narrow channel (minimum width of 14 km) located between the Iberian Peninsula and Africa.

Measurements were taken in the three stations that form the marine time series GIFT (Gibraltar Fixed Time series), which are distributed along the longitudinal axis of the SoG, i.e. G1 (5° 58.60 W, 35° 51.68 N), G2 (5° 44.75 W, 35° 54.71 N), and G3 (5° 22.10 W, 35° 59.19 N) (Figure 1) (Flecha et al., 2019).

The sampling procedure at each station in all campaigns was analogous, including the initial acquisition of temperature-salinity (T-S) profiles through a Seabird 911 Plus CTD probe installed in an oceanographic rosette. Based on the vertical thermohaline structure of the water column, the two opposite water flows were identified with the aim of taking samples in each of them by means of Niskin bottles fitted in the rosette. Therefore, samples were collected at different depths depending on the position of the flow layers in each station, covering from the surface (5 metres) to the sea bottom (360 in G1, 330 in G2 and 880 metres in G3).

Due to the absence of discrete measurements for the years 2016 and 2017, extensive data from a mooring line located at station G1 were used to complete the time series. The line is equipped with autonomous devices, including a Seabird SBE37-SMP and sensors for the continuous recording of pH and partial pressure of CO_2 (SAMI-pH and SAMI-pCO_2, Sunburst Sensors, LLC) (Flecha et al., 2015). Previous studies have shown a good agreement between data acquired by these probes and those obtained from discrete measurements in the water column, which allowed us to complement the cruises database with records provided by the SAMI devices (Seidel et al., 2008; Okazaki et al., 2017; Sánchez-Noguera et al., 2018; García-Lafuente et al., 2021).

2.2 Biogeochemical measurements

Because of the conservative property of alkalinity (Figure 1S for the SoG), this parameter was used to calculate Ω along with pH, salinity, temperature and inorganic nutrients (phosphate and silicate). For total alkalinity (TA) analysis, water was collected from the Niskin bottles in a 500 ml borosilicate bottle that was poisoned with 100 µl of $HgCl_2$ saturated aqueous solution. Measurements were performed with a Titroprocessor (model Metrohm 794 from 2005 to 2020 and model Metrohm 888 for 2021 samples) following Mintrop et al. (2000). Accuracy of TA measurements was checked by analysis of Certified Reference

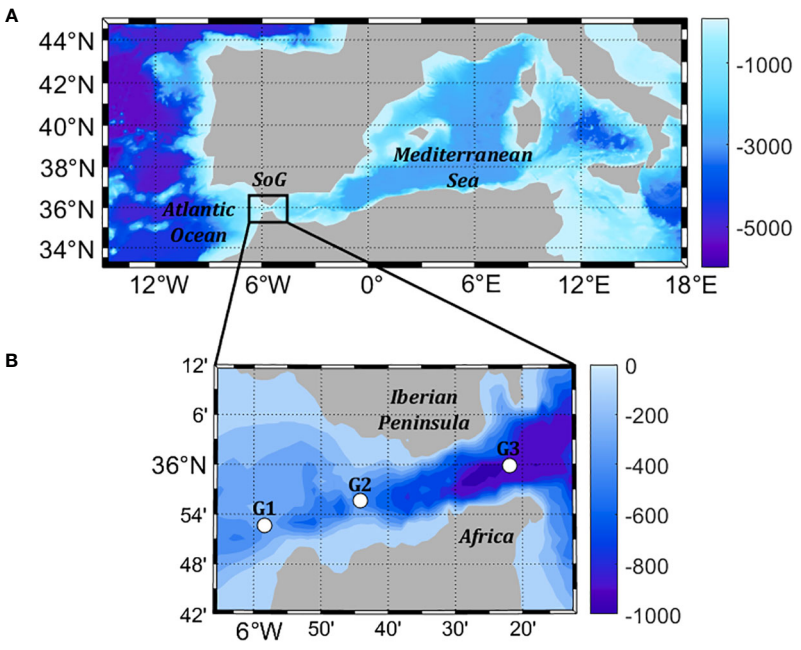

FIGURE 1
Study area. **(A)** Location of the Strait of Gibraltar. **(B)** Position of the sampling stations that form the GIFT time series (G1, G2, and G3). Topography is shown on a blue scale.

Materials provided by Prof. Andrew Dickson, Scripps Institution of Oceanography, La Jolla, CA, USA (CRMs, batches #94, #97, #136, #182, #184, #196, #199). Mean precision and accuracy of measurements in the time series were ±1 and ±4 µmol·kg^{-1}, respectively. For pH analysis, water was collected from Niskin bottles in 10 cm path-length optical glass cells for pH analysis, stored in an incubator at a temperature of 25°C, which was connected to a circulating ultrathermostat (model P. Selecta 6000383). When the samples were tempered, pH was measured in a spectrophotometer (model Shimadzu UV-2401PC), following Clayton and Byrne (1993), thereby being referred to total scale (pH_{T25}). The precision and accuracy of the method were checked through pH measurements of the above mentioned CRMs, with the original pH_{T25} value of each batch being calculated using the CO2SYS programme (Version v3.2.0 for MATLAB) (Van Heuven et al., 2011; Sharp et al., 2020), based on their nutrients, salinity and TA values provided by the supplier. Mean precision and accuracy of the pH_{T25} measurements in the time series were equivalent to ±0.0049 and ±0.0055, respectively. For nutrient determination, water was taken from Niskin bottles, filtered through 0.7 µm Whatman GF/F filters and stored frozen (-20°C) in duplicate in 5 ml plastic tubes until analysis in the laboratory that was carried out with a continuous flow auto-analyzer (Technicon) using standard colorimetric techniques Hansen and Koroleff (1999), with a precision higher than ±3%. More details regarding sample collection and biogeochemical measurements are described elsewhere (Flecha et al., 2012; Flecha et al., 2019).

$[CO_3^{2-}]$ was subsequently calculated for each sample with the CO2SYS programme using TA, pH_{T25}, phosphate and silicate concentrations, S, T, and P as input parameters. Proper dissociation constants for carbonic acid (Mehrbach et al., 1973; Dickson and Millero, 1987), stability constant of hydrogen sulfate ion (Perez and Fraga, 1987) and equilibrium constant of hydrogen fluorine (Dickson, 1990) were considered, and the boron to chlorinity ratio of Lee et al. (2010) being also used.

2.3 Determination of water masses

In order to discriminate the three water masses present in the area, the approach applied previously by Flecha et al. (2012) was used, which considers known values of potential temperature (θ) and salinity (S) to properly identify each water body (García Lafuente et al., 2007). However, marked changes in the thermohaline properties of Mediterranean water masses have been documented from 2013 onwards (García-Lafuente et al., 2021), which led us to select different values of θ and S for the period of measurements comprised between 2013 and 2021. In particular, from 2005 to 2012 the values of θ and S defining each water mass were chosen as 15.0°C and 36.2 for the NACW, 13.22°C and 38.56 for the LIW and 12.80°C and 38.45 for the WMDW (García Lafuente et al., 2007), whereas from 2013 to 2021, these values changed to 16°C and 36.20 for the NACW, 13.42°C and 38.57 for the LIW, and 12.90°C and 38.45 for the WMDW (García-Lafuente et al., 2021).

2.4 Calculation of archetypal concentrations

Archetypal annual concentrations of each variable (pCO_2, pH_{T25}, $[CO_3^{2-}]$, $\Omega_{Aragonite}$, and $\Omega_{Calcite}$) were obtained for each year and each water mass (Flecha et al., 2019). The annual archetypal concentration of a parameter N in a water mass *i* (in this case, NACW, LIW or WMDW) can be obtained through Equation 3:

$$\langle N_i \rangle = \frac{\sum_j x_{ij} N_j}{\sum_j x_{ij}} \quad (3)$$

Where N_j represents the archetypal concentration of N in sample j, and x_{ij} is the value obtained in the proportion of the water mass *i* of sample j, that is, the water mass mixing weighted average concentration in each water mass (Álvarez-Salgado et al., 2013). The standard deviation (SD) of the annual archetypal concentrations was calculated using Equation 4:

$$SD_{N_i} = \frac{\sqrt{\sum_j x_{ij} (N_j - \langle N_i \rangle)^2}}{\sum_j x_{ij}} \quad (4)$$

2.5 Determination of temporal trends, projected future changes and statistics

Temporal trends for each carbon parameter from 2005 to 2021 were determined by linear regression from the plots representing annual archetypal concentrations vs time (Flecha et al., 2019), with the standard errors also calculated and provided (Table 1).

In addition, a projection of future changes in Ω was made following the procedure described by García-Ibáñez et al. (2021) by extrapolation of the linearized Ω values and atmospheric CO_2 concentration assuming thermodynamic equilibrium conditions between atmospheric CO_2 and seawater. The hydrodynamics of SoG where physical processes clearly condition biological activity and where the influence of coastal processes is negligible (Macías et al., 2009) allow to consider that the main factor affecting Ω was the rise in CO_2. Although the response of ocean chemistry to the increase in atmospheric CO_2 is not linear for long periods of time, it can be linearised if natural logarithm (*ln*) is applied to both Ω and atmospheric CO_2 values (García-Ibáñez et al., 2021). Therefore, the future evolution of Ω in relation to the increase in atmospheric CO_2 levels in the SoG was assessed by performing a linear extrapolation of the observed relationship between *ln* Ω versus *ln* $[CO_2]_{atm}$. Our future projections are then based on the linear extrapolation of observed trends in Ω over 17 years (2005-2021). Annual averages of atmospheric CO_2 concentrations for this time period were obtained from the Izaña Global Atmospheric observatory (Agencia Estatal de Meteorología, AEMET) belonging to the NOAA (National Oceanic and Atmospheric Administration, USA) monitoring network (https://gml.noaa.gov/ccgg/trends/data.html). From the projected

10.3389/fmars.2023.1196938

Ω trends, the years in which Ω will exhibit critical or corrosive values for calcification in the water masses of the SoG was determined considering the SSP5-8.5 IPCC AR6 scenario, which assumes that CO_2 emissions in 2050 will roughly double from current levels (IPCC et al., 2021) (Figure 2S). MATLAB programming language (The MathWorks, Inc.) was used to perform the statistical analyses. Significance levels were set at $p<0.001$ or $p<0.05$ (Tables 1–3).

TABLE 1 Rates of variation of pCO_2, pH_{T25}, $[CO_3^{2-}]$, $\Omega_{Aragonite}$, and $\Omega_{Calcite}$ in the water masses present in the Strait of Gibraltar obtained from the temporal evolution of their annual archetypal concentrations during the period 2005– 2021.

Parameter	Water Masses	Slope	SE	R^2	*p*-Value
pCO_2 ($\mu atm \cdot yr^{-1}$)	NACW	3.13	± 0.46	0.81	<0.001
	WMDW	2.24	± 0.31	0.80	<0.001
	LIW	1.58	± 0.33	0.64	<0.001
pH_{T25} (pH units yr^{-1})	NACW	-0.0030	± 0.0003	0.88	<0.001
	WMDW	-0.0019	± 0.0003	0.79	<0.001
	LIW	-0.0012	± 0.0002	0.67	<0.001
$[CO_3^{2-}]$ ($\mu mol \cdot kg^{-1} \cdot yr^{-1}$)	NACW	-0.89	± 0.14	0.80	<0.001
	WMDW	-0.62	± 0.17	0.50	<0.05
	LIW	-0.32	± 0.08	0.53	<0.05
$\Omega_{Aragonite}$ (yr^{-1})	NACW	-0.0139	± 0.0024	0.75	<0.001
	WMDW	-0.0102	± 0.0019	0.69	<0.001
	LIW	-0.0080	± 0.0013	0.74	<0.001
$\Omega_{Calcite}$ (yr^{-1})	NACW	-0.0215	± 0.0034	0.78	<0.001
	WMDW	-0.0161	± 0.0029	0.70	<0.001
	LIW	-0.0129	± 0.0021	0.75	<0.001

Standard Errors are also given and denoted by SE.

TABLE 2 Statistics of linear fitting of $\Omega_{Aragonite}$ and $\Omega_{Calcite}$ vs the variation of the atmospheric CO_2 concentration in the water masses present in the Strait of Gibraltar.

Linear fitting	Water Masses	Slope	SE	R^2	*p*-Value
$\Omega_{Aragonite}$ vs $[CO_2]_{atm}$	NACW	-0.0060	± 0.0010	0.75	<0.001
	WMDW	-0.0044	± 0.0008	0.71	<0.001
	LIW	-0.0035	± 0.0005	0.77	<0.001
$\Omega_{Calcite}$vs $[CO_2]_{atm}$	NACW	-0.0092	± 0.0015	0.78	<0.001
	WMDW	-0.0070	± 0.0012	0.72	<0.001
	LIW	-0.0056	± 0.0008	0.78	<0.001

Standard Errors are denoted by SE.

TABLE 3 Statistics of future projections of $\Omega_{Aragonite}$ and $\Omega_{Calcite}$ in the water masses present in the Strait of Gibraltar.

Linear fitting	Water Masses	Slope	SE	R^2	*p*-Value
$\ln(\Omega_{Aragonite})$ vs $\ln([CO_2]_{atm})$	NACW	-0.8722	± 0.1521	0.75	<0.001
	WMDW	-0.6924	± 0.1235	0.71	<0.001
	LIW	-0.5379	± 0.0820	0.77	<0.001
$\ln(\Omega_{Calcite})$ vs $\ln([CO_2]_{atm})$	NACW	-0.8712	± 0.1402	0.78	<0.001
	WMDW	-0.7044	± 0.1228	0.72	<0.001
	LIW	-0.5583	± 0.0826	0.78	<0.001

Standard Errors are denoted by SE.

3 Results

3.1 Trends of biogeochemical variables

Figure 2 shows the trends of the archetypical concentrations of carbonate system parameters relevant for Ω in the SoG, whereas their calculated rates of change are indicated in Table 1. Overall, NACW exhibited the highest rates of change in all variables in contrast to the LIW in which variations were less pronounced over time. In particular, seawater pCO_2 progressively increased over the 2005-2021 period in all the water masses, with the NACW being characterized by the highest rise at a rate of 3.13 ± 0.46 µatm·yr^{-1}, followed by the WMDW and LIW with increasing rates of 2.24 ± 0.31 µatm·yr^{-1} and 1.58 ± 0.33 µatm·yr^{-1}, respectively. In contrast, and as expected, the rest of properties (pH_{T25}, [CO_3^{2-}], $\Omega_{Aragonite}$, and $\Omega_{Calcite}$) exhibited an opposite temporal trend, gradually decreasing over the time series.

In the NACW, pH_{T25} declined at a rate of -0.0030 ± 0.0003 pH units yr^{-1}, whereas in the WMDW and LIW pH_{T25} diminished and rates of -0.0019 ± 0.0003 and -0.0012 ± 0.0002 pH units yr^{-1} respectively. In the case of [CO_3^{2-}], temporal decreases occurred at rates of -0.89 ± 0.14 µmol·kg^{-1}·yr^{-1}, -0.62 ± 0.17 µmol·kg^{-1}·yr^{-1} and -0.32 ± 0.08 µmol·kg^{-1}·yr^{-1} in the NACW, WMDW, and LIW respectively. Accordingly, $\Omega_{Aragonite}$ lowered at rates of -0.0139 ± 0.0024 yr^{-1} in the NACW, -0.0102 ± 0.0019 yr^{-1} in the WMDW, and -0.0080 ± 0.0013 yr^{-1} in the LIW. Despite calcite being less soluble than aragonite in seawater, rates of variation of its saturation state over time were slightly greater, yet similar, than those of aragonite in the three water masses (Table 1).

3.2 Current and future evolution of saturation states of calcium carbonate minerals in the SoG

As expected, $\Omega_{Aragonite}$ and $\Omega_{Calcite}$ were negatively correlated with respect to the variation of the atmospheric CO_2 concentration ($[CO_2]_{atm}$) (Figure 3). It is evident that Ω decreased for both minerals in the area during the study period, with significant correlations always found between the contrasted parameters (p<0.001 Table 2).

Using the current rising rate of $[CO_2]_{atm}$ and annual archetypal values of $\Omega_{Aragonite}$ and $\Omega_{Calcite}$ obtained each year in the three water masses, long-term trends were projected (Figure 4). By using the correlations found between the *ln* of Ω and $[CO_2]_{atm}$ (Table 3), the $[CO_2]_{atm}$ at which critical (Table 4) and undersaturation Ω values (Table 5) will be reached in the NACW, WMDW, and LIW (Figure 2S) were estimated.

According to our analysis, unfavourable or critical conditions for calcifiers to use aragonite ($\Omega_{Aragonite}$=1.5) in the NACW, WMDW, and LIW will occur at atmospheric CO_2 concentrations of 786, 849 and 1092 ppm respectively, which are expected for years 2074, 2079, and 2096 under the SSP5-8.5 scenario, respectively (Figure 4 and Figure 2S). Undersaturation in the three water masses would arise at $[CO_2]_{atm}$ of 1251, 1524 and 2320 ppm, levels that will be reached well beyond 2100. As IPCC models do not project future trends for the next century, the exact timing for the SoG region to be undersaturated with respect to aragonite was not calculated. This is also the case for calcite, whose Ω=1.5 in the NACW, WMDW and LIW would occur at atmospheric levels of 1299, 1564 and 2312

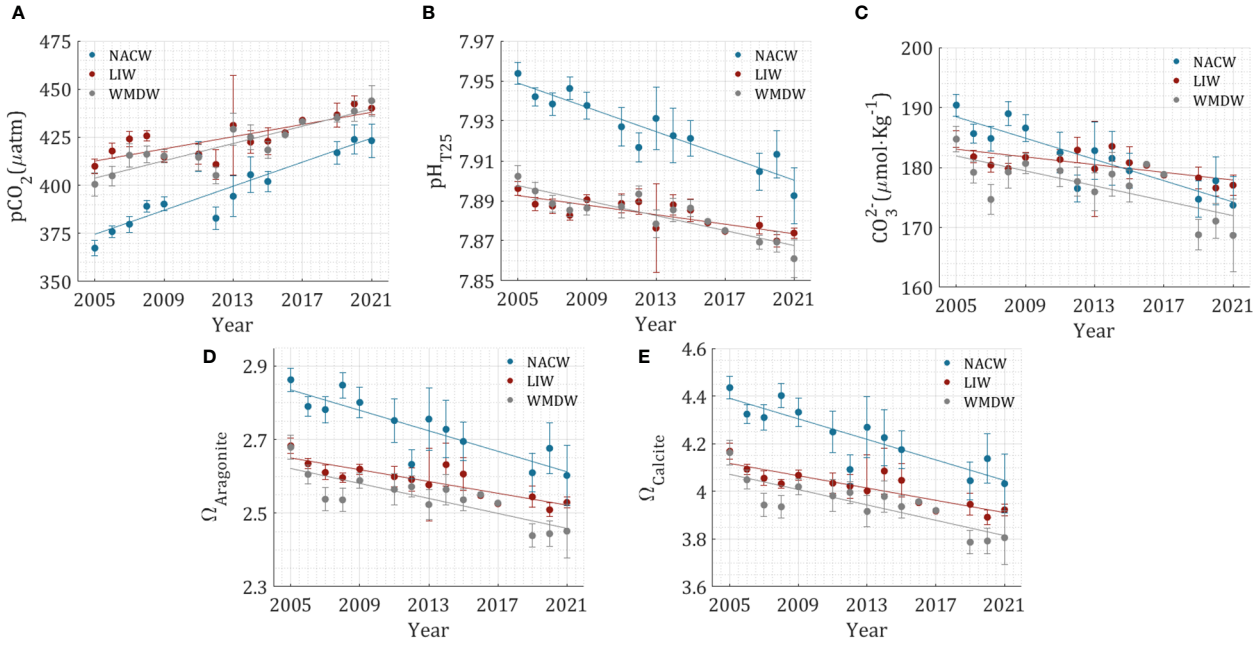

FIGURE 2
Temporal trends (2005-2021) of carbonate system parameters related to the saturation state of calcium carbonate minerals in the Strait of Gibraltar. All parameters are shown for the three water masses present in the water column that are plotted in different colours (blue, red and grey for NACW, LIW and WMDW, respectively). Data correspond to annual archetypal concentrations of pCO_2 (µatm) **(A)**; pH_{T25} **(B)**; [CO_3^{2-}] (µmol·kg^{-1}) **(C)**; $\Omega_{Aragonite}$ **(D)** and $\Omega_{Calcite}$ **(E)**.

10.3389/fmars.2023.1196938

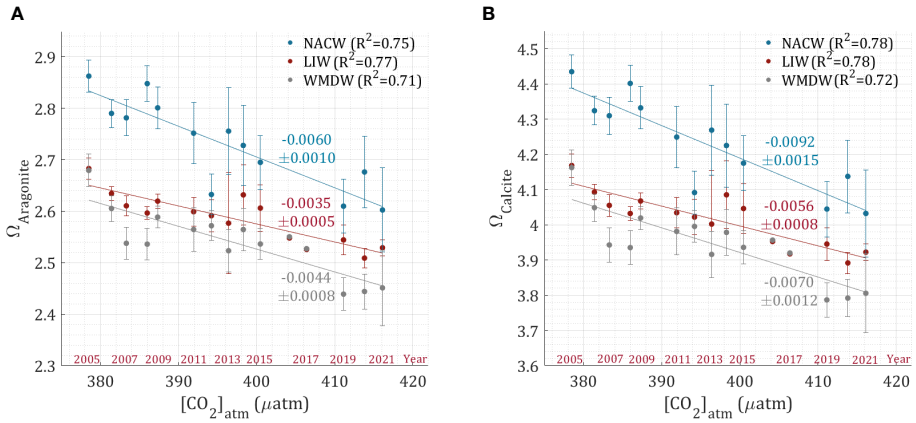

FIGURE 3
Correlation between the annual mean archetypal concentrations of the saturation state (Ω) of calcium carbonate minerals (aragonite in **(A)** and calcite in **(B)**) and annual atmospheric CO_2 concentration ($[CO_2]_{atm}$) in water masses found in the SoG, (NACW in blue, LIW in red and WMDW in grey). Slopes, SE (both in ppm^{-1}) and correlation coefficients are indicated inside the plots. The time frame is indicated as years over the X axis (in red).

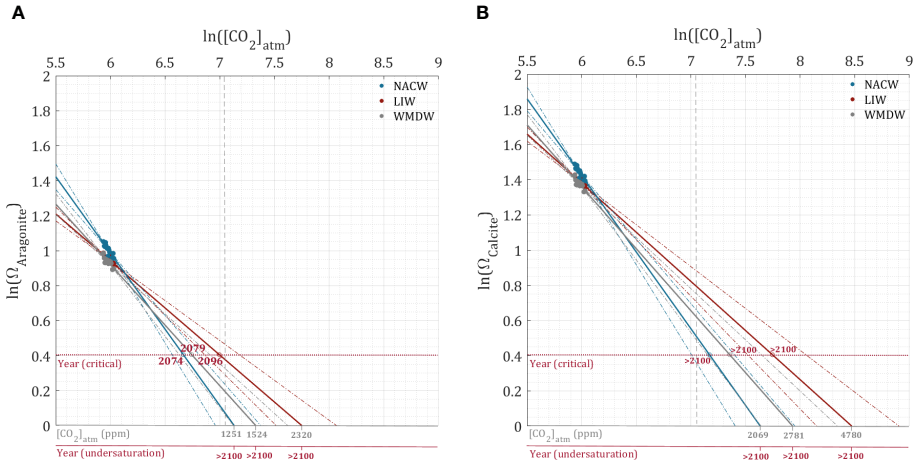

FIGURE 4
Projections of the observed long-term trends (2005-2021) of the natural logarithm of aragonite saturation state **(A)** and calcite saturation state **(B)** versus the natural logarithm of the atmospheric CO_2 concentration during the monitoring period per water mass. Solid lines represent the weighted linear trends of ln ($\Omega_{Aragonite}$) **(A)** and ln ($\Omega_{Calcite}$) **(B)** vs ln $[CO_2]_{atm}$ (upper x-axes), and dashed lines represent the error of the estimate. Lower x-axes (in grey) represent the $[CO_2]_{atm}$ values (in ppm) corresponding to the ln $[CO_2]_{atm}$ given on the upper x-axes in which undersaturation (Ω value=1) of aragonite and calcite are reached. Lower x-axes (in red) denote the years when these concentrations will occur in each water mass. The horizontal dashed line represents the Ω critical point for both minerals (value=1.5) that mark unfavourable conditions for biogenic calcification to proceed along with the years at which it is expected to appear in the three water masses. The plot is split by a grey dashed line that marks the different chemical conditions expected in all water masses with respect to Ω values before the end of the current century (on the left) and beyond 2100 (on the right) according to the SSP5-8.5 scenario.

ppm, which are not contemplated to be reached before the end of the current century under the SSP5-8.5.

The range of $[CO_2]_{atm}$ obtained by considering the errors of these estimates is shown in Tables 4 and 5 for critical and undersaturation conditions, respectively. Similarly, the range of years is summarized in Tables 2S and 3S.

4 Discussion

Results shown here show clear evidence that the saturation state of calcium carbonate minerals in the water column of the SoG is decreasing due to the decline in carbonate ions in response to the gradual diminution of seawater pH in the area. Our findings are coherent with a previous study reporting that water masses in the SoG were markedly affected by the uptake and storage of anthropogenic CO_2 during the 2005-2015 decade, leading to an evident OA in them (Flecha et al., 2019). In this work, when the time series of measurements spanned six additional years (up to 2021), the temporal decline in pH_{T25} in Mediterranean and Atlantic water masses is maintained at nearly the same annual rates as those provided by Flecha et al. (2019). Furthermore, our analysis also indicates that even though the LIW is experiencing a certain increase in its CO_2 content over time, it is less affected by the

10.3389/fmars.2023.1196938

TABLE 4 Range of $[CO_2]_{atm}$ obtained by considering the errors of the estimate for Ω =1.5 for the three water masses present in the water column.

Ω Critical	Water Masses	$[CO_2]_{atm}$ Y2= (m − SE) · X + n2	$[CO_2]_{atm}$ Y= m · X + n	$[CO_2]_{atm}$ Y1= (m + SE) · X + n1
$\Omega_{Aragonite}$	NACW	710	786	908
	WMDW	756	849	1001
	LIW	955	1092	1310
$\Omega_{Calcite}$	NACW	1102	1299	1631
	WMDW	1276	1564	2090
	LIW	1842	2312	3142

Where Y= m - X + n is the fitted line (Y= Ln(Ω); m= slope; X= Ln($[CO_2]$); n= y-intercept), whereas Y2= (m - SE) - X + n2 and Y1= (m + SE) - X + n1 are the fitted lines that consider the confidence interval of the initial fit (SE).

TABLE 5 Range of $[CO_2]_{atm}$ obtained by considering the errors of the estimate for Ω =1 for the three water masses present in the water column.

Ω Undersaturation	Water Masses	$[CO_2]_{atm}$ Y2= (m − SE) · X + n2	$[CO_2]_{atm}$ Y= m · X + n	$[CO_2]_{atm}$ Y1= (m + SE) · X + n1
$\Omega_{Aragonite}$	NACW	1055	1251	1595
	WMDW	1243	1524	2042
	LIW	1837	2320	3188
$\Omega_{Calcite}$	NACW	1646	2069	2841
	WMDW	2083	2781	4196
	LIW	3468	4781	7368

Where Y= m - X + n is the fitted line (Y= Ln(Ω); m= slope; X= Ln($[CO_2]$); n= y-intercept), whereas Y2= (m - SE) - X + n2 and Y1= (m + SE) - X + n1 are the fitted lines that consider the confidence interval of the initial fit (SE).

process of OA in relation to its Mediterranean counterpart and the NACW. As suggested by several authors, its age and intermediate position in the water column prevent a high penetration of atmospheric CO_2, which makes it more biogeochemically stable (Hassoun et al., 2015 and references therein). Nevertheless, it still contains a large natural component of CO_2 due to remineralization and/or mixing with water masses having higher anthropogenic carbon content during the long transit from its origin basin towards the Strait (Flecha et al., 2019; Vecchioni et al., 2023), which impacts its pH. OA rates have been measured in a number of marine eco-regions from coastal to open ocean regions, resulting in a broad range of values. Carstensen and Duarte (2019) provided an average acidification rate for the coastal ocean equivalent to ±0.023 pH units yr^{-1} versus a range of -0.0004 pH units yr^{-1} and -0.0026 pH units yr^{-1} in open ocean areas. If the bulk of pH data available in the water column at the SoG are considered, the average value for pH_{T25} decline in the region equals to -0.002 pH units yr^{-1}, falling within the range found for open ocean sites (Carstensen and Duarte, 2019). Certain areas are characterized by a strong pH decline tendency, such as the coastal ocean in Korea, the continental shelf of the Gulf of Cádiz, and surface waters of the Mediterranean Sea. In contrast, lower acidification rates have been reported in the North Pacific Ocean, the Munida and the Iceland Sea time series, and the upper water column (~75 m) of the Western Mediterranean. In the Atlantic time series ESTOC, BATS, and CARIACO, the rates are of the same order of magnitude as those observed in several sections of the MedSea (Table 6). Acidification rates calculated here in the water masses exchanging at the SoG (-0.0030, -0.0019 and -0.0012 pH units yr^{-1} for the NACW, the WMDW and the LIW, respectively) are in agreement with those provided in other Atlantic and Mediterranean regions. However, pH decline in the NACW seems to be slighter higher than others, which is the outcome of the conjunction between the anthropogenic CO_2 concentration contained by this water mass (Flecha et al., 2019) and the accumulation of CO_2 resulting from organic matter degradation in the productive Gulf of Cádiz (Navarro et al., 2006; Flecha et al., 2019; Álvarez-Salgado et al., 2020).

As a result of the different OA rates observed, the current saturation state of $CaCO_3$ minerals in water masses at the SoG markedly differs. It is well known that Ω varies regionally and distinct values of this parameter have been provided in the Atlantic Ocean (Fernández-Guallart, 2015; Jiang et al., 2015), the Gulf of Cádiz (Jiménez-López et al., 2021), the MedSea (Hassoun et al., 2015), the southeastern Yellow Sea (Choi et al., 2020), the northern Gulf of Alaska (Evans et al., 2013), and others (Feely et al., 2009). Our Ω estimates are of the same order of magnitude as those shown in these studies, and similar to previous calculations provided for several Mediterranean water masses (Hassoun et al., 2015; Hassoun et al., 2019). Data collected in an earlier survey (2013) carried out in

10.3389/fmars.2023.1196938

TABLE 6 Seawater pH trend values calculated in different ocean sites and time series.

Area	pH decline rate (pH units yr^{-1})	Reference
Korean Coastal ocean	-0.01	Park and Lee (2023)
Continental shelf of the Gulf of Cádiz	-0.009	Jiménez-López et al., 2021
Surface waters of the Mediterranean Sea	-0.009	Hassoun et al. (2019)
North Pacific Ocean	-0.001	Wakita et al. (2013)
Munida time series	-0.0013	Bates et al. (2014)
Iceland Sea	-0.0014	Bates et al. (2014)
Surface waters of the Western Mediterranean	-0.0013	Hassoun et al. (2022)
Atlantic sites	-0.0016 to -0.0025	Bates and Peters (2007) Santana-Casiano et al. (2007) Bates et al. (2012) Bates et al. (2014) Takahashi et al. (2014) Bates and Johnson, 2020
Eastern Mediterranean Basin	-0.0021 to -0.0024	Hassoun et al. (2022)
Western Mediterranean Basin	-0.0013 to -0.0022	Hassoun et al. (2022) Fourrier et al. (2022)
Central Mediterranean	-0.0016	Fourrier et al. (2022)
Strait of Gibraltar	-0.002	This work

the SoG, provided values of $\Omega_{Aragonite}$ and $\Omega_{Calcite}$ of ~2.6-3 and ~4.2-4.6, respectively (Hassoun et al., 2015), in agreement with our results. Similarly, $\Omega_{Aragonite}$ of approximately 2.5 has been given for the $NACW_T$ (North Atlantic Central Water of subtropical origin) at the Gulf of Cádiz using data taken from 2014 to 2016 (Jiménez-López et al., 2021), which is not far from our calculations based on 17 continuous years of measurements in the SoG (Figure 2). This study also reported $\Omega_{Aragonite}$ values of 1.56 for the $NACW_P$ (North Atlantic Central Water of subpolar origin) and 2.22 for the MOW, which is much lower than omega shown here for the Mediterranean outflow at the Strait. Moreover, in the Levantine Basin, average values of $\Omega_{Aragonite}$ and $\Omega_{Calcite}$ equivalent to 3.4 and 5.3 have been obtained elsewhere, corresponding to a recently formed LIW (Hassoun et al., 2015).

Our assessment also shows a gradual temporal reduction of Ω in the three water masses over the time series. Overall, $\Omega_{Aragonite}$ decreased at annual rates of -0.0107 yr^{-1} in the whole water column of the Strait, -0.0091 yr^{-1} in the MOW and at specific rates of -0.0139 yr^{-1}, -0.0102 yr^{-1} and -0.0080 yr^{-1}, in the NACW, WMDW and LIW, respectively (Table 4S). These rates are much lower than those reported in the continental shelf of the Gulf of Cádiz (-0.0552 yr^{-1}, Jiménez-López et al., 2021) using disperse measurements from 2006 to 2016 and in 2013 in the Levantine basin (-0.07 yr^{-1}, Hassoun et al., 2019). Our results are, however, in line with several studies conducted across the Atlantic that provide values comprised between -0.010 yr^{-1} and -0.0140 yr^{-1} (González-Dávila et al., 2010; Bates et al., 2012; Takahashi et al., 2014; Fontela et al., 2021). In the case of calcite, the rates of decline (-0.0168 yr^{-1}, -0.0145 yr^{-1}, -0.0215 yr^{-1}, -0.0161 yr^{-1} and -0.0129 yr^{-1} in the water column, the MOW, NACW, WMDW and LIW, respectively) are also similar to those computed in Atlantic time series (values between -0.010 yr^{-1} and -0.0209 yr^{-1}, Bates and Peters, 2007; González-Dávila et al., 2010; Takahashi et al., 2014; Bates and Johnson, 2020) but lower than that in the Levantine basin (-0.1 yr^{-1}, Hassoun et al., 2019).

Spatial variations in the ranges of calcium carbonate mineral decline can be attributed to the fact that every region and each water mass has specific characteristics that directly influence the rate of change of Ω. For instance, coastal areas and marginal seas generally have a higher tendency to acidify as a result of stronger anthropogenic impacts (Carstensen and Duarte, 2019). Additionally, a significant increase in temperature and biological factors are also associated (Jiménez-López et al., 2021). In contrast, in most open ocean areas, the influence of the biological uptake of CO_2 decreases and the change in saturation of calcium carbonate minerals is mostly caused by the uptake of atmospheric CO_2 (García-Ibáñez et al., 2021).

Considering the rates of $\Omega_{Aragonite}$ decline in the SoG and taking the IPCC AR6 SSP5-8.5 scenario for the CO_2 emissions progression, a high vulnerability of calcifiers to ocean acidification is expected in the area before the end of the 21st century. In particular, critical conditions for biogenic calcification will be reached in less than 60 years in the upper and bottom layers of the SoG (51 and 56 years for the NACW and WMDW respectively). Furthermore, even though the LIW seems to be less strongly perturbated than the other two water masses, an unfavourable scenario for calcification would also occur in approximately 75 years from now. Due to the lower solubility of calcite in seawater (Sulpis et al., 2022), unfavourable conditions with respect to this mineral will arise in the region beyond 2100. Critical conditions have been defined here by a

threshold of Ω=1.5 for both aragonite and calcite, as this value has been adopted in several studies to assess the vulnerability of marine calcifiers to OA and its repercussion for marine ecosystems (Gruber et al., 2012; Broadgate et al., 2013; Ekstrom et al., 2015; Zhai, 2018). Moreover, evident reductions in calcification rates of marine organisms have been reported at Ω values of 2-3.5 (Guinotte et al., 2003; Yamamoto et al., 2012; Eyre et al., 2018). Therefore, the range of current estimations of $\Omega_{Aragonite}$ in the SoG along with its projected rates of decline in all the water masses under a high CO_2 emission pathway depict a catastrophic scenario for the marine ecosystem in the region. Calcifiers are essential to maintain the ecological status of the pelagic and benthic ecosystems (and their living resources) in the sub-basins connected by the Strait, the Gulf of Cádiz and the Mediterranean Alboran Sea (Vertino et al., 2010; Movilla, 2015; Lozano et al., 2020), where a significant number of planktonic calcifiers (coccolithophores, foraminifera), pelagic mollusks (pteropods), bivalves, calcareous algae and corals thrive (Reguera et al., 2009; Bautista-Chamizo et al., 2016; Jiménez-López et al., 2021). According to our findings, regional calcifying communities are at high risk due to the gradual OA that is proceeding in the area, which will restrict the levels of carbonate ions required for a proper calcification well before the end of the 21st century.

It has been predicted that by 2100, 91% of the whole ocean will be undersaturated to aragonite (Gattuso et al., 2015) including the Southern Ocean and parts of the North Pacific (Feely et al., 2009), the Irminger and Iceland Basin (García-Ibáñez et al., 2021), the Nordic Seas (Fransner et al., 2022), the polar Surface water (Matear and Lenton, 2014) and the lower NACW in the Western Atlantic (Fernández-Guallart, 2015). This scenario would co-occur with critical conditions in certain eco-regions, such as the tropical oceans, where survival of coral reefs will be compromised by the availability of carbonate to form aragonite (Matear and Lenton, 2014). Although undersaturation of calcite in the surface ocean is expected beyond the end of the 21st century (Feely et al., 2009), levels of this mineral will be greatly reduced with respect to current concentrations. Therefore, the trends found in a choke oceanographic spot, such as the SoG, after almost two decades of observations, support the concern about the impact of the pH decline on marine ecosystems. Maintenance of ocean observing systems is then essential to establish baselines required to document and predict the vulnerability of marine ecosystems to climate change and provide tools for efficiently developing and implementing adaptation and mitigation strategies.

Data availability statement

The original contributions presented in the study are publicly available. This data can be found here: https://doi.org/10.20350/digitalCSIC/14556.

Author contributions

SA-V: Data curation, Formal analysis, Investigation, Methodology, Software, Writing – original draft; SF: Data curation, Formal analysis, Methodology, Software, Supervision, Validation, Writing - review & editing; FP: Conceptualization, Methodology, Formal analysis, Writing - review & editing; GN: Methodology, Funding acquisition; JG-L: Funding acquisition, Data curation, Methodology, Writing - review & editing; AM: Data curation, Resources; IEH: Conceptualization, Data curation, Funding acquisition, Investigation, Methodology, Resources, Supervision, Validation, Writing – review & editing.

Funding

This work was supported by the European projects CARBOOCEAN (FP6-511176), CARBOCHANGE (FP7-264879), PERSEUS (FP7-287600), Eurosea and COMFORT. The EuroSea (Improving and integrating the European Ocean Observing and Forecasting System) and COMFORT (Our common future ocean in the Earth system - quantifying coupled cycles of carbon, oxygen, and nutrients for determining and achieving safe operating spaces with respect to tipping points) projects have received funding from the European Union's Horizon 2020 research and innovation programme under grant agreements No 862626 and 820989, respectively. Funding from the Junta de Andalucia through the TECADE grant (PY20_00293) is also acknowledged. SA-V was supported by a pre-doctoral grant FPU19/04338 from the Spanish Ministry of Science, Innovation and Universities. FP was supported by the BOCATS2 (PID2019-104279GB-C21) project funded by MCIN/AEI/10.13039/501100011033. This work is a contribution to the CSIC Interdisciplinary Thematic Platform OCEANS+, funded by the European Union-Next Generation EU Agreement between MITECO, CSIC, AZTI, SOCIB, and the universities of Vigo and Cadiz, to promote research and generate scientific knowledge in the field of marine sustainability. SF acknowledges the financial support of a "Vicenç Munt Estabilitat" postdoctoral contract from the Balearic Islands Government and the PTA2018–015585-I funded by the Spanish Ministry of Science and Innovation.

Acknowledgments

We would like to thank the crews of all the research vessels involved in this study. We would also like to thank María Ferrer, Angélica Enrique, Silvia Rayo, Antonio Moreno, and David Roque for the collection and analysis of samples. We also thank Martha B. Dunbar for English language revision.

Conflict of interest

The authors declare that the research was conducted in the absence of any commercial or financial relationships that could be construed as a potential conflict of interest.

Publisher's note

All claims expressed in this article are solely those of the authors and do not necessarily represent those of their affiliated organizations, or those of the publisher, the editors and the reviewers. Any product that may be evaluated in this article, or claim that may be made by its manufacturer, is not guaranteed or endorsed by the publisher.

Supplementary material

The Supplementary Material for this article can be found online at: https://www.frontiersin.org/articles/10.3389/fmars.2023.1196938/full#supplementary-material

References

Álvarez-Salgado, X. A., Nieto-Cid, M., Álvarez, M., Pérez, F. F., Morin, P., and Mercier, H. (2013). New insights on the mineralization of dissolved organic matter in central, intermediate, and deep water masses of the northeast North Atlantic. *Limnology Oceanography* 58 (2), 681–696.

Álvarez-Salgado, X. A., Otero, J., Flecha, S., and Huertas, I. E. (2020). Seasonality of dissolved organic carbon exchange across the Strait of Gibraltar. *Geophysical Res. Lett.* 47 (18), e2020GL089601.

Bates, N. R., Best, M. H. P., Neely, K., Garley, R., Dickson, A., and Johnson, R. (2012). Detecting anthropogenic carbon dioxide uptake and ocean acidification in the North Atlantic Ocean. *Biogeosciences* 9 (7), 2509–2522.

Bates, N. R., Astor, Y. M., Church, M. J., Currie, K. I., Dore, J. E., Gonzalez-Davila, M., et al. (2014). A time-series view of changing surface ocean chemistry due to ocean uptake of anthropogenic CO_2 and ocean acidification. *Oceanography* 27 (1), 126–141. doi: 10.5670/oceanog.2014.16

Bates, N. R., and Johnson, R. J. (2020). Acceleration of ocean warming, salinification, deoxygenation and acidification in the surface subtropical North Atlantic Ocean. *Commun. Earth Environ.* 1 (1), 33.

Bates, N. R., and Peters, A. J. (2007). The contribution of atmospheric acid deposition to ocean acidification in the subtropical North Atlantic Ocean. *Mar. Chem.* 107 (4), 547–558.

Bautista-Chamizo, E., Romano de Orte, M., DelValls, A., and Riba, I. (2016). Simulating CO_2 leakages from CCS to determine Zn toxicity using the marine microalgae Pleurochrysis roscoffensis. *Chemosphere* 144, 955–965.

Broadgate, W., Riebesell, U., Armstrong, C., Brewer, P., Denman, K., Feely, R., et al. (2013). "Ocean acidification: summary for policymakers'. *Third Symposium on the ocean in a high-CO_2 world*. Int. Geosphere-Biosphere Programme: Stockholm, Sweden, 24 pp.

Carstensen, J., and Duarte, C. M. (2019). Drivers of pH variability in coastal ecosystems. *Environ. Sci. Technol.* 53 (8), 4020–4029.

Choi, Y., Cho, S., and Kim, D. (2020). Seasonal variation in aragonite saturation states and the controlling factors in the southeastern Yellow Sea. *Mar. pollut. Bull.* 150, 110695.

Clayton, T. D., and Byrne, R. H. (1993). Spectrophotometric seawater pH measurements: total hydrogen ion concentration scale calibration of m-cresol purple and at-sea results. *Deep-Sea Res. Part I* 40 (10), 2115–2129. doi: 10.1016/0967-0637(93)90048-8

Dickson, A. G. (1990). Standard potential of the reaction: $AgCl(s) + 12H_2(g) = Ag(s) + HCl(aq)$, and and the standard acidity constant of the ion HSO_4^- in synthetic sea water from 273.15 to 318.15 K. *J. Chem. Thermodynamics* 22 (2), 113–127. doi: 10.1016/0021-9614(90)90074-Z

Dickson, A. G., and Millero, F. J. (1987). A comparison of the equilibrium constants for the dissociation of carbonic acid in seawater media. *Deep Sea Res. Part A Oceanographic Res. Papers* 34 (10), 1733–1743. doi: 10.1016/0198-0149(87)90021-5

Doney, S. C., Fabry, V. J., Feely, R., and Kleypas, J. (2009). Ocean acidification: the other CO_2 problem. *Annu. Rev. Mar. Sci.* 1, 169–192.

Doney, S. C., Busch, D. S., Cooley, S. R., and Kroeker, K. J. (2020). The impacts of ocean acidification on marine ecosystems and reliant human communities. *Annu. Rev. Environ. Resour.* 45, 83–112.

Ekstrom, J. A., Suatoni, L., Cooley, S. R., Waldbusser, G. G., Cinner, J., Ritter, J., et al. (2015). Vulnerability and adaptation of US shellfisheries to ocean acidification. *Nat. Climate Change* 5 (3), 207–214.

Evans, W., Mathis, J. T., Winsor, P., Statscewich, H., and Whitledge, T. T. (2013). A regression modeling approach for studying carbonate system variability in the northern Gulf of Alaska. *J. Geophysical Research: Oceans* 118 (1), 476–489.

Eyre, B. D., Cyronak, T., Drupp, P. S., De Carlo, E., Sachs, J. P., and Andersson, A. J. (2018). Coral reefs will transition to net dissolving before end of century. *Science* 359 (6378), 908–911.

Feely, R. A., Doney, S. C., and Cooley, S. R. (2009). Ocean acidification: Present conditions and future changes in a high-CO_2 world. *Oceanography* 22 (4), 36–47.

Feely, R. A., Chris, S., Byrne, R., Millero, F. J., Dickson, A., Wanninkhof, R. , et al. (2012). Decadal changes in the aragonite and calcite saturation state of the Pacific Ocean. *Global Biogeochemical Cycles* 26 (3). doi: 10.1029/2011GB004157

Fernández-Guallart, E. (2015). *Spatiotemporal variability of the carbonate system in the North Atlantic Ocean*. Universidad de Las Palmas de Gran Canaria: Instituto de Ciencias del Mar (ICM) e Instituto de Investigaciones Marinas (IIM)-Consejo Superior de Investigaciones Científicas (CSIC).

Flecha, S., Pérez, F. F., Navarro, G., Ruiz, J., Olivé, I., Rodriguez-Galvez, S., et al. (2012). Anthropogenic carbon inventory in the Gulf of Cádiz. *J. Mar. Syst.* 92 (1), 67–75. doi: 10.1016/j.jmarsys.2011.10.010

Flecha, S., Pérez, F. F., García-Lafuente, J., Sammartino, S., Rios, A. F., and Huertas, I. E. (2015). Trends of pH decrease in the Mediterranean Sea through high frequency observational data: indication of ocean acidification in the basin. *Sci. Rep.* 5 (1), 1–8.

Flecha, S., Pérez, F. F., and Huertas, I. E. (2019). Decadal acidification in Atlantic and Mediterranean water masses exchanging at the Strait of Gibraltar. *Sci. Rep.* 9 (1), 1–11. doi: 10.1038/s41598-019-52084-x

Fontela, M., Pérez, F. F., Carracedo, L. I., Padin, X. A., Anton, V., García-Ibáñez, M. I., et al. (2020). The Northeast Atlantic is running out of excess carbonate in the horizon of cold-water corals communities. *Sci. Rep.* 10 (1), 1–11. doi: 10.1038/s41598-020-71793-2

Fontela, M., Velo, A., Gilcoto, M., and Pérez, F. F. (2021). Anthropogenic CO_2 and ocean acidification in Argentine Basin Water Masses over almost five decades of observations. *Sci. Total Environ.* 779, 146570.

Fourrier, M., Coppola, L., D'Ortenzio, F., Migon, C., and Gattuso, J.-P. (2022). Impact of intermittent Convection in the northwestern Mediterranean Sea on Oxygen content, Nutrients and the Carbonate system. *J. Geophysical Research: Oceans* 127 (9), e2022JC018615. doi: 10.1029/2022JC018615

Fransner, F., Fröb, F., Tjiputra, J., Goris, N., Lauvset, S. K., Skjelvan, I., et al. (2022). Acidification of the nordic seas. *Biogeosciences* 19 (3), 979–1012.

Friedlingstein, P., O'Sullivan, M., Jones, M. W., Andrew, R. M., Gregor, L., Hauck, J., et al. (2022). Global carbon budget 2022. *Earth System Sci. Data* 14 (4), 1917–2005.

Gačić, M., Schroeder, K., Civitarese, G., Cosoli, S., Vetrano, A., and Borzelli, G. L. E. (2013). Salinity in the Sicily Channel corroborates the role of the Adriatic–Ionian Bimodal Oscillating System (BiOS) in shaping the decadal variability of the Mediterranean overturning circulation. *Ocean Sci.* 9 (1), 83–90.

García-Ibáñez, M. I., Bates, N. R., Bakkler, D. C. E., Fontela, M., and Velo, A. (2021). Cold-water corals in the Subpolar North Atlantic Ocean exposed to aragonite undersaturation if the 2° C global warming target is not met. *Global Planetary Change* 201, 103480.

García-Lafuente, J., et al. (2007). Recent observations of seasonal variability of the Mediterranean outflow in the Strait of Gibraltar. *J. Geophysical Research: Oceans* 112 (C10005). doi: 10.1029/2006JC003992

García-Lafuente, J., Sanchez-Roman, A., Diaz del Rio, G., Sannino, G., Sánchez-Garrido, J. C., and V, J. D. R. (2021). Hotter and weaker mediterranean outflow as a response to basin-wide alterations. *Front. Mar. Sci.* 8, 613444. doi: 10.3389/fmars.2021.613444

Gattuso, J.-P., Magnan, A., Billé, R., Cheung, W., Howes, E., and Joos, F. (2015). Contrasting futures for ocean and society from different anthropogenic CO_2 emissions scenarios. *Science* 349 (6243), aac4722. doi: 10.1126/science.aac4722

Gledhill, D. K., White, M., Salisbury, J., Thomas, H., Mlsna, I., Liebman, M., et al. (2015). Ocean and coastal acidification off New England and Nova Scotia. *Oceanography* 28 (2), 182–197. doi: 10.5670/oceanog.2015.41

González-Dávila, M., Santana-Casiano, J. M., González Rueda, M. J., and Llinás, O. (2010). The water column distribution of carbonate system variables at the ESTOC site from 1995 to 2004. *Biogeosciences* 7 (10), 3067–3081.

Gruber, N., Hauri, C., Lachkar, ., Loher, D., Frölicher, T. L., and Plattner, G.-K. (2012). Rapid progression of ocean acidification in the California Current System. *Science* 337 (6091), 220–223. doi: 10.1126/science.1216773

Gruber, N., Bakker, D. C. E., DeVries, T., Gregor, L., Hauck, J., Landschützer, P., et al. (2023). Trends and variability in the ocean carbon sink. *Nat. Rev. Earth Environ.* 4 (2), 119–134. doi: 10.1038/s43017-022-00381-x

Guinotte, J. M., Buddemeier, R. W., and Kleypas, J. A. (2003). Future coral reef habitat marginality: temporal and spatial effects of climate change in the Pacific basin. *Coral reefs* 22, 551–558.

Hansen, H. P., and Koroleff, F. (1999). Determination of nutrients. *Methods Seawater Anal.* Third Edition. Chapter 10, 159–228. doi: 10.1002/9783527613984.ch10

Hassoun, A. E. R., Gemayel, E., Krasakopoulou, E., Goyet, C., Saab, M. A-A., Guglielmi, V., et al. (2015). Deep-Sea Research I Acidification of the Mediterranean Sea from anthropogenic carbon penetration. *Deep-Sea Res. Part I* 102, 1–15. doi: 10.1016/j.dsr.2015.04.005

Hassoun, A. E. R., Fakhri, M., Raad, N., Saab, M. A-A., Gemayel, E., and De Carlo, E. H. (2019). Deep-Sea Research Part II The carbonate system of the Eastern-most Mediterranean Sea, Levantine Sub-basin : Variations and drivers. *Deep-Sea Res. Part II* 164 (March), 54–73. doi: 10.1016/j.dsr2.2019.03.008

Hassoun, A. E. R., Bantelman, A., Canu, D. M., Comeau, S., Chales, G., Gattuso, J-P., et al. (2022). Ocean acidification research in the Mediterranean Sea: Status, trends and next steps. *Front. Mar. Sci.* 9. doi: 10.3389/fmars.2022.892670

Heinze, C., Blenckner, T., Martins, H., Rusiecka, D., Döscher, R., Gehlen, M., et al. (2021). The quiet crossing of ocean tipping points. *PNAS118* 9), e2008478118. doi: 10.1073/pnas.2008478118

Impacts, A. (2014). *Vulnerability. Part A: global and sectoral aspects. Contribution of working group II to the fifth assessment report of the intergovernmental panel on climate change* (Cambridge, United Kingdom and New York, NY, USA: Cambridge University Press).

IPCC, Masson-Delmotte, V., Zhai, P., Pirani, A., Connors, S. L., Péan, C., et al. (2021). *Climate change 2021: the physical science basis. Contribution of working group I to the sixth assessment report of the intergovernmental panel on climate change.* (Cambridge: Press).

Jiang, L., Feely, R., Carter, B. R., Greeley, D. J., Gledhill, D. K., and Arzayus, K. M. (2015). Climatological distribution of aragonite saturation state in the global oceans. *Global Biogeochemical Cycles* 29 (10), 1656–1673.

Jiménez-López, D., Ortega, T., Sierra, A., Ponce, R., Gómez-Parra, A., and Forja, J. (2021). Aragonite saturation state in a continental shelf (Gulf of Cádiz, SW Iberian Peninsula): Evidences of acidification in the coastal area. *Sci. Total Environ.* 787, 147858. doi: 10.1016/j.scitotenv.2021.147858

Kroeker, K. J., Kordas, R., Crim, R. N., Hendriks, I., Ramajo, L., Singh, G., et al. (2013). Impacts of ocean acidification on marine organisms: Quantifying sensitivities and interaction with warming. *Global Change Biol.* 19 (6), 1884–1896. doi: 10.1111/gcb.12179

Lascaratos, A. (1993). Estimation of deep and intermediate water mass formation rates in the Mediterranean Sea. *Deep Sea Res. Part II: Topical Stud. Oceanography* 40 (6), 1327–1332.

Lee, K., Kim, T-W., Byrne, R., Millero, F. J., Feely, R., and Liu, Y-M. (2010). The universal ratio of boron to chlorinity for the North Pacific and North Atlantic oceans. *Geochimica Cosmochimica Acta* 74 (6), 1801–1811.

Le Quéré, C., Moriarty, R., Andrew, R. M., Canadell, J. G., Sitch, S., Korsbakken, J. I., et al. (2015). Global carbon budget 2015. *Earth System Sci. Data* 7 (2), 349–396.

Lozano, P., Fernández Salas, L. M., Hernández-Molina, F. J., Sánchez, R. F. L., Sánchez Guillamón, O., et al. (2020). Multiprocess interaction shaping geoforms and controlling substrate types and benthic community distribution in the Gulf of Cádiz. *Mar. Geology* 423, 106139.

Macías, D., Navarro, G., Bartual, A., Echevarría, F., and Huertas, I. E. (2009). Primary production in the Strait of Gibraltar: Carbon fixation rates in relation to hydrodynamic and phytoplankton dynamics. *Estuarine Coast. Shelf Sci.* 83 (2), 197–210.

Matear, R. J., and Lenton, A. (2014). Quantifying the impact of ocean acidification on our future climate. *Biogeosciences* 11 (14), 3965–3983. doi: 10.5194/bg-11-3965-2014

Mathesius, S., Hofmann, M., Caldeira, K., and Schellnhuber, H. J. (2015). Long-term response of oceans to CO_2 removal from the atmosphere. *Nat. Climate Change* 5 (12), 1107–1113.

MEDOC Group, T. (1970). Observation of formation of deep water in the Mediterranean Sea 1969'. *Nature* 227 (5262), 1037–1040.

Mehrbach, C., Culberson, C. H., Hawley, J. E., and Pytkowick, R. M. (1973). Measurement of the apparent dissociation constants of carbonic acid in seawater at atmospheric pressure. *Limnology Oceanography* 18 (6), 897–907. doi: 10.4319/lo.1973.18.6.0897

Melzner, F., Mark, F. C., Seibel, B., and Tomanek, L. (2020). Ocean acidification and coastal marine invertebrates: tracking CO_2 effects from seawater to the cell. *Annu. Rev. Mar. Sci.* 12, 499–523. doi: 10.1146/annurev-marine-010419-010658

Miller, A. W., Reynolds, A. C., Sobrino, C., and Riedel, G. F. (2009). Shellfish face uncertain future in high CO_2 world: influence of acidification on oyster larvae calcification and growth in estuaries. *PloS One* 4 (5), e5661.

Mintrop, L., Pérez, F. F., González-Dávila, M., Santana-Casiano, J. M., and Körtzinger, A. (2000). Alkalinity determination by potentiometry: Intercalibration using three different methods. *Ciencias Marinas* 26 (1), 23–27. doi: 10.7773/cm.v26i1.573

Mostofa, K. M. G., Liu, C-Q., Zhai, W. D., Minella, M., Vione, D., Gao, K., et al. (2016). Reviews and Syntheses: Ocean acidification and its potential impacts on marine ecosystems. *Biogeosciences* 13 (6), 1767–1786. doi: 10.5194/bg-13-1767-2016

Movilla, J. I. (2015). *Effects of ocean acidification on mediterranean corals*. Universidad de Las Palmas de Gran Canaria. Instituto de Ciencias del Mar (ICM)-Consejo Superior de Investigaciones Científicas (CSIC).

Navarro, G., Ruiz, J., Huertas, I. E., García, C. M., Criado-Aldeanueva, F., and Echevarría, F. (2006). Basin-scale structures governing the position of the deep fluorescence maximum in the Gulf of Cádiz. *Deep Sea Res. Part II: Topical Stud. Oceanography* 53 (11–13), 1261–1281.

Okazaki, R. R., Sutton, A. J., Feely, R. A., Dickson, A., Alin, S., Chris, A., et al. (2017). Evaluation of marine pH sensors under controlled and natural conditions for the Wendy Schmidt Ocean Health XPRIZE. *Limnology Oceanography: Methods* 15 (6), 586–600.

Orr, J. C., Fabry, V. J., Aumont, O., Bopp, L., Doney, S. C., Feely, R. A., et al. (2005). Anthropogenic ocean acidification over the twenty-first century and its impact on calcifying organisms. *Nature* 437 (7059), 681–686. doi: 10.1038/nature04095

Pan, T. C. F., Applebaum, S. L., and Manahan, D. T. (2015). Experimental ocean acidification alters the allocation of metabolic energy. *Proc. Natl. Acad. Sci. United States America* 112 (15), 4696–4701. doi: 10.1073/pnas.1416967112

Park, G.-H., and Lee, S.-E. (2023). *Significant changes in pH and saturation state of calcium carbonate in coastal ocean waters in Korea* (Copernicus Meetings). EGU23-12184. General Assembly 2023. doi: 10.5194/egusphere-egu23-12184

Perez, F. F., and Fraga, F. (1987). Association constant of fluoride and hydrogen ions in seawater. *Mar. Chem.* 21 (2), 161–168.

Pörtner, H.-O., Karl, D. M., Boyd, P. W., Cheung, W., Lluch-Cota, S. E., Nojiri, Y., et al. (2014). "Ocean systems," in *Climate change 2014: impacts, adaptation, and vulnerability. Part A: global and sectoral aspects. contribution of working group II to the fifth assessment report of the intergovernmental panel on climate change* (Cambridge University Press), 411–484. doi: 10.1017/CBO9781107415379.011

Raven, J., Caldeira, K., Elderfield, H., Hoegh-Guldberg, O., Liss, P., Riebesell, U., et al. (2005). *Ocean acidification due to increasing atmospheric carbon dioxide.* (The Royal Society).

Reguera, D. F., Riba, I., Forja, J. M., and DelValls, A. (2009). An integrated approach to determine sediment quality in areas above CO_2 injection and storage in agreement with the requirements of the international conventions on the protection of the marine environment. *Ecotoxicology* 18 (8), 1123–1129.

Riebesell, U., Zondervan, I., Rost, B., Tortell, P. D., Zeebe, R. E., and Morel, F. M. M. (2000). Reduced calcification of marine plankton in response to increased atmospheric CO_2. *Nature* 407 (6802), 364–366. doi: 10.1038/35030078

Roether, W., Birgit, K., Klein, B., Beitzel, V., and Manca, B. B. (1998). Property distributions and transient-tracer ages in Levantine Intermediate Water in the Eastern Mediterranean. *J. Mar. Syst.* 18 (1–3), 71–87.

Sánchez-Noguera, C., Lange, I. D., Cortés, J., Jimenez, C., Morales, A., Wild, C., et al. (2018). Natural ocean acidification at Papagayo upwelling system (north Pacific Costa Rica): implications for reef development. *Biogeosciences* 15 (8), 2349–2360.

Santana-Casiano, J. M., Gonzalez-Davila, M., De José, M. J., Llinás, O., and González-Dávila, E. (2007). The interannual variability of oceanic CO_2 parameters in the northeast Atlantic subtropical gyre at the ESTOC site. *Global Biogeochemical Cycles* 21 (1), 1015. doi: 10.1029/2006GB002788

Sarmiento, J. L., and Gruber, N. (2002). Sinks for anthropogenic carbon. *Phys. Today* 55 (8), 30–36. doi: 10.1063/1.1510279

Seidel, M. P., DeGrandpre, M. D., and Dickson, A. G. (2008). A sensor for in *situ* indicator-based measurements of seawater pH. *Mar. Chem.* 109 (1–2), 18–28.

Sharp, J. D., Pierrot, D., Humphreys, M. P., Epilaton, J.-M., Orr, J. C., Lewis, E. R., et al. (2020). CO2SYSv3 For MATLAB. *Zenodo* 2020. doi: 10.5281/ZENODO.3950563

Silverstein, T. P. (2022). Rising atmospheric carbon dioxide could doom ocean corals and shellfish: simple thermodynamic calculations show why. *J. Chem. Educ.* 99 (5), 2020–2025.

Sulpis, O., Agrawal, P., Wolthers, M., Munhoven, G., Walker, M., and Middelburg, J. J. (2022). Aragonite dissolution protects calcite at the seafloor. *Nat. Commun.* 13 (1), 1104.

Takahashi, T., Sutherland, S. C., Chipman, D. W., Goddard, J. G., Ho, C., and Newberger, T. (2014). Climatological distributions of pH, pCO_2, total CO_2, alkalinity, and $CaCO_3$ saturation in the global surface ocean, and temporal changes at selected locations. *Mar. Chem.* 164, 95–125.

Van Heuven, S., Pierrot Rae, J. W. B., Lewis, E., and Wallace, D. W. R. (2011). *MATLAB program developed for CO_2 System Calculations. ORNL/CDIAC-105b. Carbon Dioxide Information Analysis Center* (Oak Ridge, Tenn: Oak Ridge Natl. Lab., US Dep. of Energy).

Vecchioni, G., Cessi, P., Pinardi, N., Rousselet, L., and Trotta, F. (2023). A Lagrangian estimate of the Mediterranean outflow's origin. *Geophysical Res. Lett.* 50, e2023GL103699. doi: 10.1029/2023GL103699

Vertino, A., Savini, A., Rosso, A., Di Geronimo, S. I., Mastrototato, F., Sanfilippo, R., et al. (2010). Benthic habitat characterization and distribution from two representative sites of the deep-water SML Coral Province (Mediterranean). *Deep Sea Res. Part II: Topical Stud. Oceanography* 57 (5–6), 380–396.

Wakita, M., Watanabe, S., Honda, M. C., Nagano, A., Kimoto, K., Matsumoto, K., et al. (2013). Ocean acidification from 1997 to 2011 in the subarctic western North Pacific Ocean. *Biogeosciences* 10 (12), 7817–7827.

Williamson, P., and Widdicombe, S. (2017). *The rise of CO_2 and ocean acidification, Encyclopedia of the Anthropocene* (Elsevier Inc) (5), 51–59. doi: 10.1016/B978-0-12-809665-9.09877-3

Yamamoto, S., Kayanne, H., Terai, M., Watanabe, A., Kato, K., Negishi, A., et al. (2012). Threshold of carbonate saturation state determined by CO_2 control experiment. *Biogeosciences* 9 (4), 1441–1450. doi: 10.5194/bg-9-1441-2012

Zhai, W. (2018). Exploring seasonal acidification in the Yellow Sea. *Sci. China Earth Sci.* 61 (6), 647–658.